Geochemistry Geophysics Geosystems G3

AN ELECTRONIC JOURNAL OF THE EARTH SCIENCES

Published by AGU and the Geochemical Society

Article

Volume 9, Number 8

6 August 2008

Q08003, doi:10.1029/2008GC001943

ISSN: 1525-2027

Assessing the ability of the ^{14}C projection-age method to constrain the circulation of the past in a 3-D ocean model

J. Franke

Department of Geosciences, University of Bremen, Klagenfurter Strasse, D-28359 Bremen, Germany (joerg.franke@palmod.uni-bremen.de)

Now at Swiss Federal Research Institute WSL, Zürcherstrasse 111, CH-8903 Birmensdorf, Switzerland

M. Schulz and A. Paul

Department of Geosciences, University of Bremen, Klagenfurter Strasse, D-28359 Bremen, Germany

Center for Marine Environmental Sciences, University of Bremen, Leobener Strasse, D-28359 Bremen, Germany

J. F. Adkins

Division of Geological and Planetary Sciences, California Institute of Technology, 1200 California Avenue, MS 100-23, Pasadena, California 91125, USA

[1] Radiocarbon differences between benthic and planktonic foraminifera (B-P ages) and radiocarbon projection ages are both used to determine changes of the past ocean circulation rate. A global 3-D ocean circulation model with a constant modern ocean circulation is used to study which method is less influenced by atmospheric $\Delta^{14}C$ variations. Three factors cause uncertainties: first, the long equilibration time of the ocean after atmospheric $\Delta^{14}C$ changes; second, different mixing processes in the ocean, which cause an ocean response of smaller amplitude than the atmospheric forcing; and third, the unknown source region and corresponding initial surface ^{14}C reservoir age of subsurface waters. The model suggests that B-P ages and projection ages have lower uncertainties the closer they are to deepwater formation zones. In the North Atlantic the B-P age method is less influenced by atmospheric $\Delta^{14}C$ variations than the projection-age method. Projections ages vary less in the Pacific as long as atmospheric $\Delta^{14}C$ decreases linearly. A more irregular atmospheric $\Delta^{14}C$ evolution leads to age variations of similar magnitude with both methods. On the basis of the model experiment, we suggest a potential improvement of the projection-age method.

Components: 7960 words, 7 figures.

Keywords: projection age; top-to-bottom age; benthic-planktonic age; radiocarbon; ocean circulation.

Index Terms: 4901 Paleoceanography: Abrupt/rapid climate change (1605); 4999 Paleoceanography: General or miscellaneous; 1105 Geochronology: Quaternary geochronology.

Received 11 January 2008; **Revised** 30 April 2008; **Accepted** 19 June 2008; **Published** 6 August 2008.

Franke, J., M. Schulz, A. Paul, and J. F. Adkins (2008), Assessing the ability of the ^{14}C projection-age method to constrain the circulation of the past in a 3-D ocean model, *Geochem. Geophys. Geosyst.*, *9*, Q08003, doi:10.1029/2008GC001943.

1. Introduction

[2] Past ocean circulation changes are a matter of active research [*Lynch-Stieglitz et al.*, 2007]. Many proxies have been developed over the last several years to draw conclusions about how ocean circulation rate differed from today, e.g., sortable silt [*McCave et al.*, 1995] or Pa/Th [*McManus et al.*, 2004]. Still, one of the most frequently used methods remains the determination of past ocean circulation rate from ^{14}C differences between planktonic and benthic foraminifera at the same depth in a sediment core [*Broecker et al.*, 1988; *Shackleton et al.*, 1988; *Duplessy et al.*, 1989]. One potential error in the benthic-to-planktonic age difference (B-P age), often called the top-to-bottom age, is the temporal change of atmospheric $\Delta^{14}C$ ($\Delta^{14}C_{atm}$) such as the irregular decrease of more than 300‰ during the last deglaciation. These $\Delta^{14}C_{atm}$ variations will be visible in the surface ocean within a few months but it will take hundreds of years until the signal reaches some parts of the deep ocean.

[3] To eliminate this source of error, *Adkins and Boyle* [1997] introduced a method which takes this circulation induced time lag into account. Three parameters are needed for the correction. First a calendar age estimate that can be derived from parallel U/Th dating in deep-sea corals or, less accurately, from reservoir effect corrected and calibrated ^{14}C measurements in planktonic foraminifera. In addition, estimates of deep water $\Delta^{14}C$ and atmospheric $\Delta^{14}C$ are required. Starting from deep sea $\Delta^{14}C$ at a given calendar age, ^{14}C decay is calculated backward through time (the projection). After a specific amount of "reverse" decay time the $\Delta^{14}C$ value of the sample reaches the $\Delta^{14}C$ level of the atmosphere. The corresponding difference between the calendar age of the deep-sea sample and the calendar age of intersection with the atmospheric curve is then corrected for the constant surface ^{14}C reservoir age of the source region to give the so-called "projection age."

[4] The projection-age method has been applied to the deep North Atlantic [*Adkins et al.*, 1998; *Skinner and Shackleton*, 2004], the northwest Pacific [*Ahagon et al.*, 2003] and the western North Atlantic [*Keigwin and Schlegel*, 2002]. However several uncertainties mentioned by *Adkins and Boyle* [1997] were never fully quantified or eliminated. The projection-age method was developed in a idealized and purely advective model that assumed direct atmosphere-ocean surface exchange without any reservoir-age effect. The deep ocean received the water from the surface after a specific amount of time (the ventilation age) using a closed system decay approach (no mixing of different water masses). Thus, the deep ocean $\Delta^{14}C$ curve nearly mimicked the atmospheric curve with a time lag of the ventilation age [see *Adkins and Boyle*, 1997, Figure 1].

[5] Uncertainties in the projection-age method arise from mixing processes in the ocean and spatial and temporal variations in the reservoir age [e.g., *Bondevik et al.*, 2006; *Hughen et al.*, 2006; *Schimmelmann et al.*, 2006]. The correction for the reservoir age is difficult because its variability has only been reconstructed for a few locations and because of the largely unknown source region where water was subducted in the past. Another problem arises from the fact that atmospheric $\Delta^{14}C$ variations can result from ocean circulation changes themselves and not just from production-rate changes [*Adkins and Boyle*, 1997]. This has been shown for the Younger Dryas [*Bondevik et al.*, 2006] and would result in an overestimation of both B-P and projection ages [*Adkins and Boyle*, 1997].

[6] We use a coupled atmosphere-ocean circulation model to investigate the relationships between ventilation, B-P, and projection ages. The goal is to provide a guideline to which method works best at a given location, to highlight advantages and disadvantages of the methods, and to explore potential improvements of the projection-age method.

2. Model Description and Simulation Setup

[7] To test the projection-age concept we used the global University of Victoria Earth System Climate Model (UVic ESCM) [*Weaver et al.*, 2001] in version 2.7. It consists of a three-dimensional ocean general circulation model (Modular Ocean Model, version 2, [*Pacanowski*, 1995]) coupled to a two-dimensional energy-moisture balance model of the atmosphere [*Fanning and Weaver*, 1996] and a dynamic-thermodynamic sea ice model [*Bitz et al.*, 2001]. The horizontal resolution of all compartments is 3.6° in longitude and 1.8° in latitude, while the ocean has 19 levels of irregular depth, increasing from 50 m at the surface to 500 m at the deepest levels [*Weaver et al.*, 2001; *Meissner et al.*, 2003]. It is driven by seasonal and latitudinal variations in solar radiation incident at the top of the atmosphere. Wind stress at the ocean surface is

prescribed from a monthly climatology [*Kalnay et al.*, 1996]. We used the option of a rotated grid to avoid convergence of the meridians near the North Pole. Subgrid-scale mixing is included following the *Gent and McWilliams* [1990] parametrization for mixing associated with mesoscale eddies. Vertical diffusion is increasing from the surface to the deep ocean [*Bryan and Lewis*, 1979].

[8] Radiocarbon was included as an additional tracer following the guidelines of the Ocean Carbon Modeling Intercomparison Project (OCMIP-2) [*Orr et al.*, 2000] in the ocean part of the model. The gas exchange with the atmosphere depends on the gradient between the atmosphere and the surface ocean, wind speed, sea-ice coverage and sea surface temperature. In the ocean the tracer is transported via diffusion and advection. A sink has been added to account for the ^{14}C decay with a half-life of 5730 years. The atmosphere is treated with respect to ^{14}C as one well-mixed box. This assumption is justified because we investigate variations of centennial to millennial timescale while the atmospheric mixing time for ^{14}C is on the order of some years.

[9] The time elapsed since seawater was last exposed to the atmosphere is referred to as "age" in tracer oceanography [*England*, 1995]. As a reference for comparison of ^{14}C age with the ocean ventilation age we added a so-called ideal age tracer [*Williams et al.*, 1995; *England*, 1995] to the model. Each time when the ideal age tracer reaches the ocean surface layer in the model it is reset to zero, assuming that it was exposed to the atmosphere when it made its way into the turbulent mixed surface layer. Below the surface layer the tracer ages, while transported and mixed like all other tracers.

[10] We ran two simulations for different atmospheric $\Delta^{14}C$ forcings using preindustrial present-day (PIPD) boundary conditions (insolation and land-ice for the year 1950 common era (C.E.) and an atmospheric CO_2 content of 280 ppmv). The first simulation was the control run with a constant $\Delta^{14}C_{atm}$ of 0‰. It should assess the model ability to calculate the present-day radiocarbon distribution in the ocean using modern boundary condition and to highlight discrepancies between the different methods.

[11] In the second experiment $\Delta^{14}C_{atm}$ is linearly decreased over 5000 years from 0 to −100‰ as done by *Adkins and Boyle* [1997] (Figure 3, model year 10,000–5000). This generally decreasing trend in $\Delta^{14}C_{atm}$ has been reconstructed for the last deglaciation [*Reimer et al.*, 2004], but of course it was not as gradual and also not monotonic. Reconstructions show plateaus of constant $\Delta^{14}C_{atm}$ as well as $\Delta^{14}C_{atm}$ increases, e.g., in the Younger Dryas. To get one step closer to such conditions, we simulated what would happen if the $\Delta^{14}C_{atm}$ increases for an interval of 1000 years by 20‰ and then decreases again afterward linearly over 4000 years to −160‰ (Figure 3, model year 5000–0). The entire 10,000-year-long simulation was started from the control run and its steady state $\Delta^{14}C$ in the atmosphere. In both experiments circulation-induced $\Delta^{14}C_{atm}$ changes were not simulated as the circulation is kept constant.

[12] The "age" terms used here are defined as follows. The reservoir age is the ^{14}C age difference between the atmosphere and the surface ocean [e.g., *Stuiver et al.*, 1986]. It is influenced by air-sea gas exchange and mixing of ^{14}C depleted water across the thermocline. By definition the Suess effect corrected ^{14}C age of the atmosphere in the year 1950 C.E. is zero [*Stuiver and Polach*, 1977]. This means the ^{14}C age of the surface ocean layer is the same as the reservoir age in the control run where a value 0‰ has been set for the atmosphere. The surface reservoir age belonging to a subsurface water parcel depends on the location where it last had contact with the atmosphere. Because this location is often unknown, especially far away from deepwater formation zones, one can choose a local value, the global low-latitude value of 400 years, or a best-guess value for the appropriate sinking region. Although the projection-age method was never intended to use a spatially varying value that included low-latitude upwelling regions, we used the local reservoir age to correct the model results for a better comparison with B-P ages. We call this "local reservoir age" while the "true reservoir age" would be the one in which the path of the water since it became subducted would be considered. The ventilation age is defined after [*Thiele and Sarmiento*, 1990] as the time elapsed since the water parcel left the surface ocean and contact with the atmosphere ("the ideal age").

[13] It should be noted that the difference between a benthic and a planktonic ^{14}C age is based on the true half life which is ∼3% larger than the Libby half life.

3. Results

3.1. Control Run

[14] The different methods to estimate circulation age are compared for constant $\Delta^{14}C_{atm}$ (=0‰)

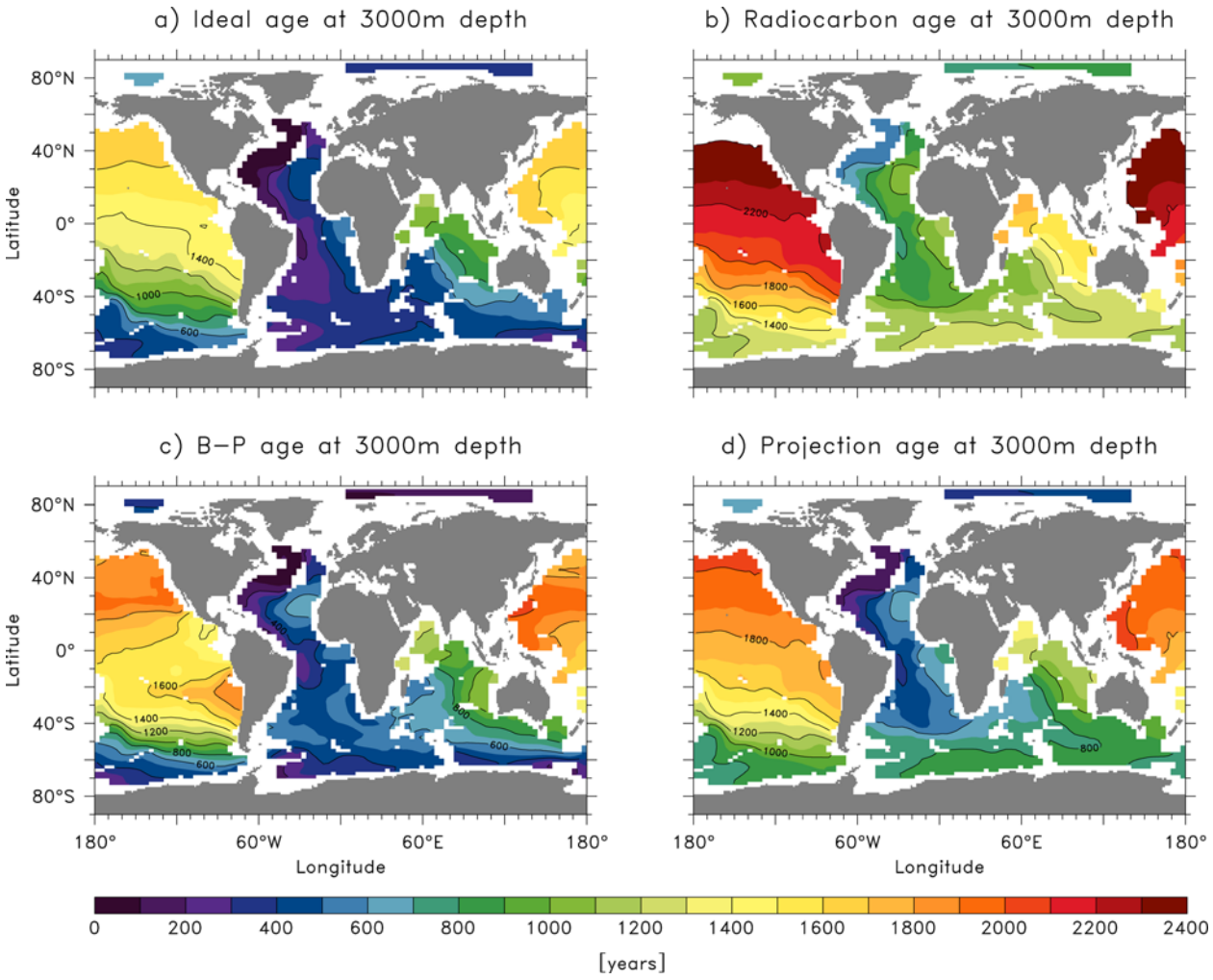

Figure 1. Maps from the simulation with constant $\Delta^{14}C_{atm}$ and PD boundary condition at 3000 m depth. (a) Modeled ideal/ventilation ages are calculated with a tracer that is always set to zero in the surface ocean layer of the model. (b) Radiocarbon ages showing how projection ages without reservoir age correction would look. They have the same pattern as the ideal ages in Figure 1a and indicate the difficulty of correcting for the true reservoir-age effect. (c) Conventional B-P ages, in this simulation nearly equal to the projection ages if they would also be corrected for a local surface reservoir age. (d) Projection ages corrected for a global mean reservoir age of 400 years.

forcing (Figure 1). A 3000 m depth level was chosen to show the ocean ventilation pattern uninfluenced by the bottom topography and above the calcite compensation depth in the Pacific [*Berger*, 1977]. The B-P ages (Figure 1c) are of similar magnitude as the ventilation ages (Figure 1a) at a global scale. Anomalies of B-P ages relative to ideal ages in the Atlantic reach up to ~200 years. In the Pacific they are up to twice as high (Figure 2a).

[15] To calculate the projection ages, the reservoir age of the source region is needed. If the local reservoir age would be assumed, projection ages would be nearly the same as B-P ages as long as $\Delta^{14}C_{atm}$ is constant (Figure 1c). In regions where surface ^{14}C ages are strongly influenced by the upwelling of old water, the local reservoir age would contradict the original idea of projection ages. An estimate of how projection ages in these regions should look like is shown in Figure 1d, in which a global mean reservoir age of 400 years has been used for correction.

[16] In the case where projection ages are not corrected for the reservoir age, they are identical to the ^{14}C ages at depth (Figure 1b), which show a pattern similar to that of the ideal ages. Obviously the missing reservoir-age correction results in greater differences relative to the ideal ages than for B-P ages. The necessary reservoir age correc-

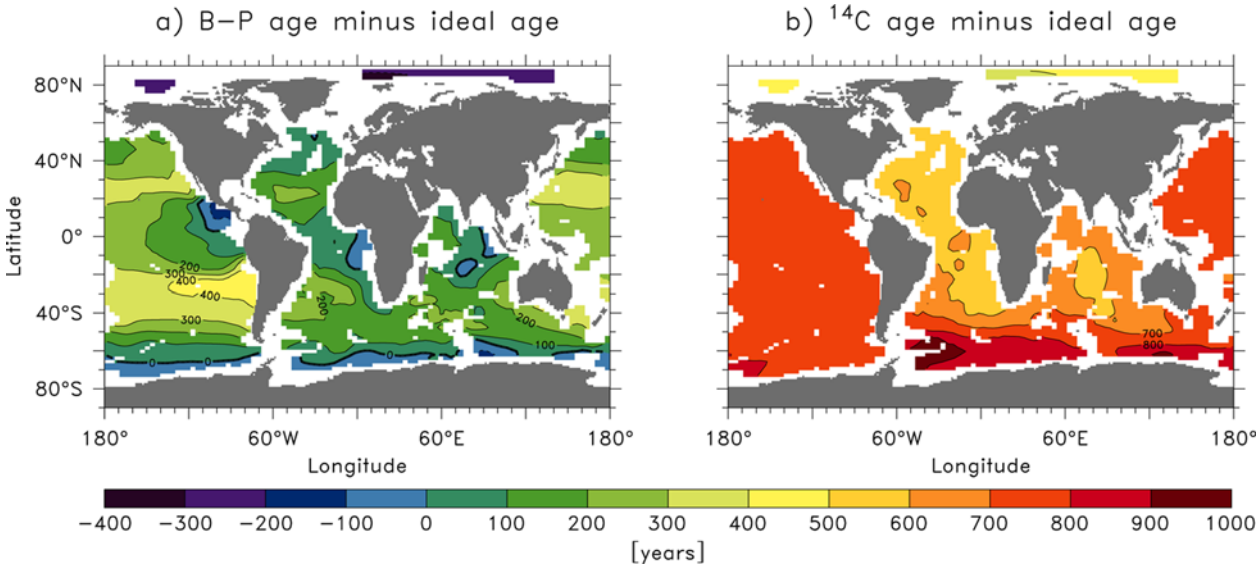

Figure 2. Anomaly maps for the control run. (a) Difference between B-P ages (Figure 1c) and ideal ages (Figure 1a). (b) Anomaly of ^{14}C ages (Figure 1b) to ideal ages (Figure 1a). Here, the anomalies indicate the reservoir age for which the projection ages need to be corrected to show the ventilation age in case of constant $\Delta^{14}C_{atm}$.

tion can be assessed in the model, as long as $\Delta^{14}C_{atm}$ is constant, from the difference plot of ideal age and the ^{14}C age (Figure 2b). The maximum offset of ~700 years can again be found in the deep Pacific.

3.2. Experiment With Decreasing Atmospheric $\Delta^{14}C$

[17] An experiment of linearly decreasing $\Delta^{14}C_{atm}$ was used by *Adkins and Boyle* [1997] to show the advantage of the projection-age method. We simulate a comparable scenario from model year 10,000 to 5000 (Phase 1 in Figures 3 and 4). The response of the ocean to the atmospheric forcing is shown at two locations in the northern Atlantic (Figure 3a) and the northern Pacific (Figure 3b) at 3000 m depth. At most other oceanic locations the $\Delta^{14}C$-evolution curves fall somewhere in between these two extremes, only the initial oceanic $\Delta^{14}C$ values, the time lag and the smoothing of the deep ocean $\Delta^{14}C$-curve varies between locations. Noteworthy is the response of the deep ocean at the beginning of the $\Delta^{14}C$ decrease. In the Atlantic it runs nearly parallel to the atmosphere, while in the Pacific, there is no sharp bend in the deep ocean $\Delta^{14}C$-curve. Instead it is a smoothed curve which reduces the difference between the subsurface ocean and the atmospheric/surface ocean $\Delta^{14}C$.

[18] The way projection ages are calculated is indicated by the colored arrows (Figure 3). Note that when comparing the temporal evolution curves in Figure 4, all curves are referenced to the time in the modeled deep ocean where the projection started. As predicted and explained by *Adkins and Boyle* [1997] for the simplified scenario of a closed-system decay, B-P ages are generally decreasing when atmospheric $\Delta^{14}C$ is decreasing (Figure 4, model year 10,000 to 5000). B-P ages always drift, even though the circulation is constant. The drift in the north Atlantic is small after the initial shift to a lower B-P age, while a faster B-P age drift continues in the Pacific as long as $\Delta^{14}C_{atm}$ decreases linearly.

[19] Projection ages, as originally proposed by *Adkins and Boyle* [1997], are calculated by finding the intersection of the ^{14}C-decay trajectory with the atmospheric $\Delta^{14}C$-evolution curve (indicated by the red arrows in Figure 3) and a subsequent correction for a constant reservoir age (dashed red arrows in Figure 3). Because of the offset between surface ocean and atmospheric $\Delta^{14}C$, the decay trajectory intersects with an atmospheric $\Delta^{14}C$ level too far back in time. At the beginning of the experiment the projection curve "catches" the flat part of the atmospheric curve while the deep-sea curve is already decreasing. The consequence is an increasing projection age at the beginning of the experiment at both locations before it slowly decreases back to the equilibrium value (Figure 4).

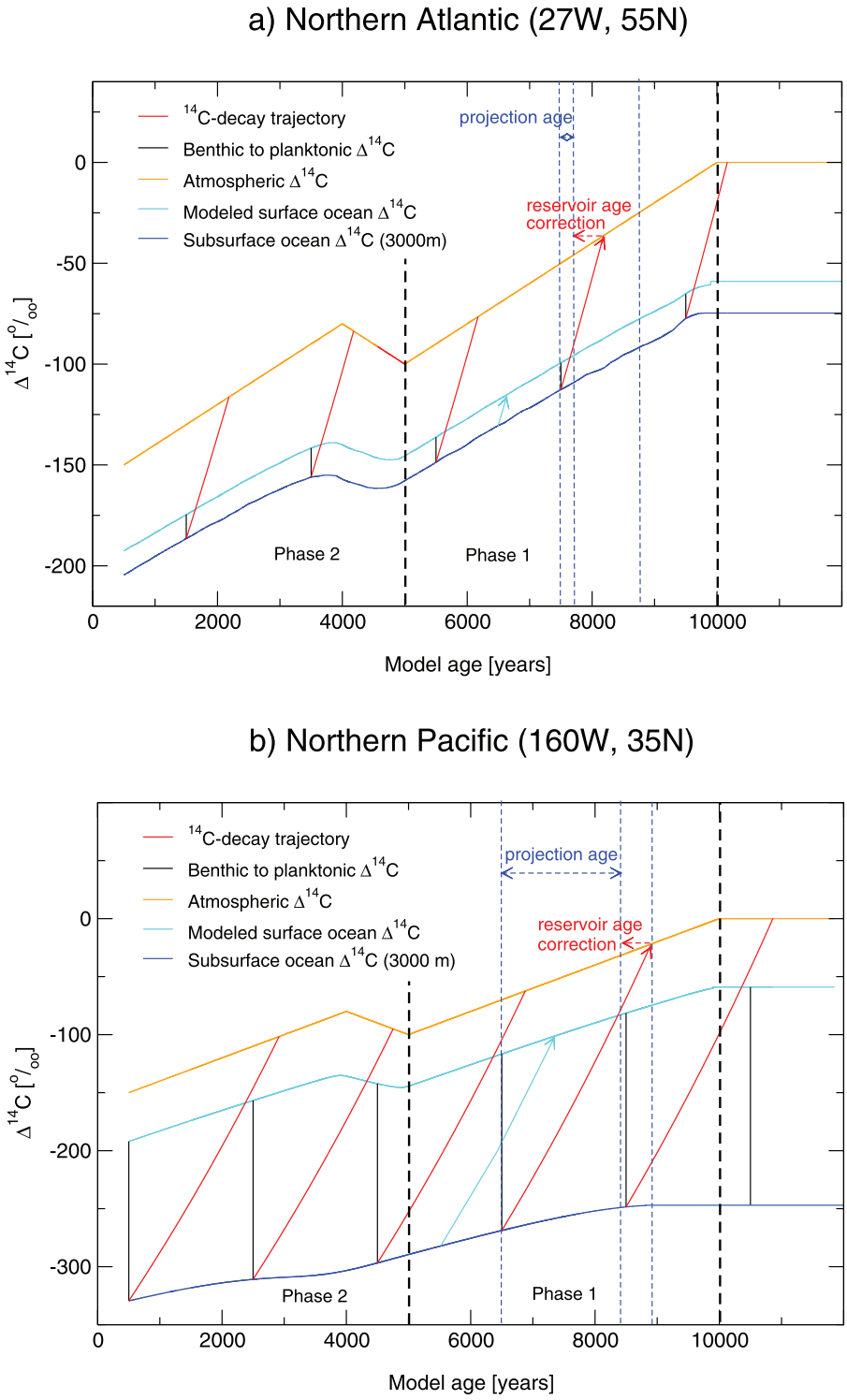

Figure 3. Response of the ocean to the $\Delta^{14}C_{atm}$ forcing at two locations: (a) the Atlantic (27W, 55N) and (b) Pacific (160W, 35N). The cyan curves show the fast response of the model's surface ocean layer to the atmospheric forcing (orange curve). The blue curves below demonstrates the slow response of the deep ocean at 3000 m depth due to ocean circulation and mixing. The original projection ages are calculated by finding the intersection of the ^{14}C-decay trajectory (red curve/arrow) with the orange atmospheric curve and a subsequent reservoir age correction (red dashed arrows). Alternatively, projection ages are calculated by building the ^{14}C-decay trajectory to the intersection with the modeled surface ocean Δ^{14}C (cyan arrow), instead of the atmospheric curve.

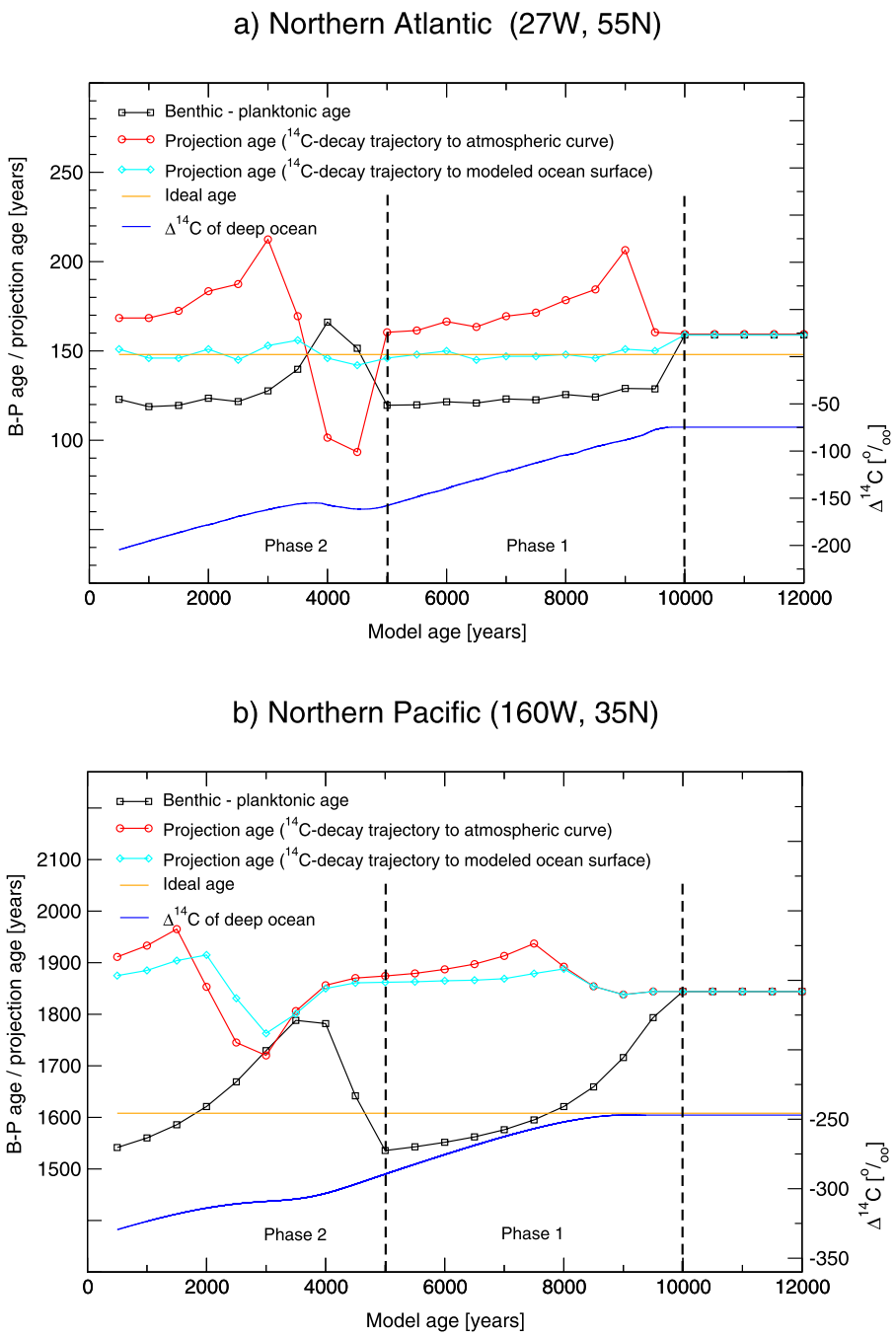

Figure 4. Temporal changes in the B-P ages and different ways to calculate projection ages, as they were indicated by the black lines and colored arrows in Figure 3. All curves are referenced to the modeled deep ocean $\Delta^{14}C_{atm}$ (blue curve). Changes in B-P ages are plotted in black, original projection ages (intersection of ^{14}C-decay trajectory with atmospheric curve and subsequent reservoir age correction) are plotted in red, and alternative projection ages (intersection of ^{14}C-decay trajectory with modeled surface ocean curve) are plotted in cyan.

[20] Additionally projection ages have been calculated by finding the intersection of a decay trajectory with the modeled surface ocean Δ^{14}C curve (cyan curve in Figure 3) at the same location. At the chosen Atlantic site the curve is similar to the B-P ages. Projection ages decrease when $\Delta^{14}C_{atm}$ starts to decrease, but the amplitude of the variations is smaller than for the B-P ages (Figure 4a). In contrast, the projection-age curve in the Pacific is similar to the original projection age method, but

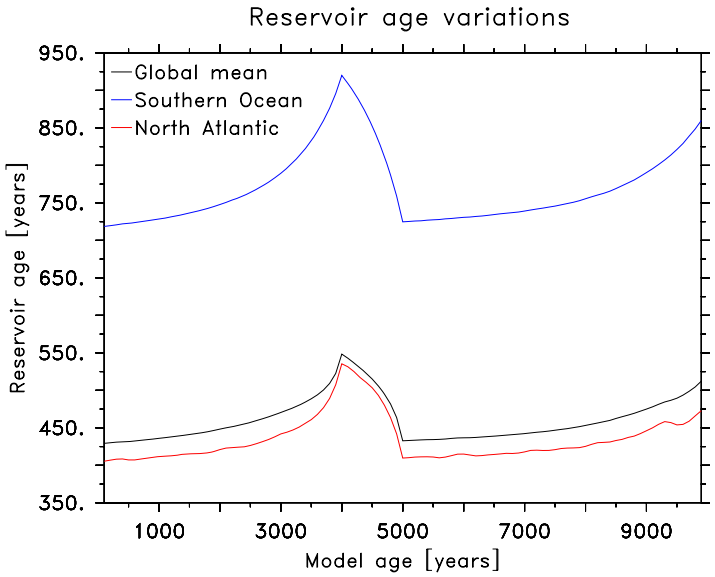

Figure 5. Global and local reservoir age variations due to atmospheric $\Delta^{14}C$ variations. The global mean reservoir age (black curve) decreases by nearly 100 years in the 5000 years of linear $\Delta^{14}C_{atm}$ decrease (model year 10,000–5000). When atmospheric $\Delta^{14}C$ increases by 20‰, the reservoir age increases rapidly by over 100 years. Corresponding to the final $\Delta^{14}C_{atm}$ decrease, reservoir ages decrease again nearly as rapidly as they increased. These rapid variations occur because of the slow response of the huge oceanic reservoir to changes in the comparable small atmospheric reservoir. In the northern North Atlantic the reservoir age variations are only slightly larger than the global mean (red curve). A much higher variability of more than 200 years of reservoir-age change occurs in the Southern Ocean (blue curve).

again the amplitude of the variations is smaller (Figure 4b).

[21] After 5000 years of linear $\Delta^{14}C_{atm}$ decrease, compared to the control run the B-P ages are ~50 years too old in the North Atlantic and about 300 years too old in the North Pacific, and both still have a decreasing trend. Projection ages, on the other hand, quickly increase by ~50 years in the North Atlantic and by ~100 years in the North Pacific, but afterward they return to the constant equilibrium value (Figure 4).

[22] Pacific projection ages are older than the ideal age and on the same level as B-P ages because the local reservoir age has been chosen. Altogether it can be noticed that both methods show age variations, which are smaller in the Atlantic and larger in the Pacific.

3.3. Experiment With 1000-Year-Long Atmospheric $\Delta^{14}C$ Increase

[23] The atmospheric $\Delta^{14}C$ increase between model year 5000 and 6000 (Phase 2 in Figures 3 and 4) is reflected in the deep Atlantic ocean, only slightly smoothed and with a small time lag with respect to the atmospheric forcing (Figure 3b). In contrast, the atmospheric $\Delta^{14}C$ peak hardly exists in the deep Pacific $\Delta^{14}C$ evolution at all. There is only a very little effect of reduced $\Delta^{14}C$ decrease visible (Figure 3a). Thus both, projection and B-P ages vary significantly over time.

[24] The evolution of surface ocean $\Delta^{14}C$ is also not parallel to the atmospheric $\Delta^{14}C$. This can be seen in the difference between the model surface $\Delta^{14}C$ (cyan curve in Figure 3) and the atmospheric $\Delta^{14}C$ (orange curve in Figure 3), indicating that reservoir ages vary rapidly in our simulation. Because of the atmospheric ^{14}C changes, the global mean reservoir age varies by ~120 years. The reservoir-age variations of 130 years in the northern North Atlantic region are of similar magnitude. In contrast, reservoir ages in the Southern Ocean show a higher variability of more than 200 years (Figure 5).

[25] Comparing projection and B-P ages, errors are shifted in time if the deep sea point is used as a reference (Figure 4). Projection ages fall by ~50 years in the Atlantic as $\Delta^{14}C_{atm}$ increases over 1000 years. Coeval to the atmospheric $\Delta^{14}C$ decrease they rapidly increase by more than 100 years. Afterward they slowly return to the equilibrium level. In the Pacific the reaction is

similar but has more than twice the amplitude and is shifted in time.

[26] B-P ages increase by ~50 years in the Atlantic and then slowly return to the constant value they had in the linear $\Delta^{14}C_{atm}$ decrease experiment. In the Pacific B-P ages increase by ~300 years before they start their decreasing trend again.

4. Discussion

4.1. Control Run

[27] Differences between projection or B-P ages and ideal or ventilation ages are caused by two factors. First deep water parcels are not simply a translation of local surface waters, or surface waters with a global mean reservoir age, to the deep ocean. Accordingly, neither the difference between the surface and subsurface ^{14}C ages nor the assumption of 400 years can eliminate the true reservoir-age effect. To arrive at a true ventilation age, the reservoir-age correction would have to be made for the region at which the subsurface water parcel had its last contact with the atmosphere. The deep Pacific Ocean, for instance, is influenced by deep water formed in the Southern Ocean with a reservoir age of well over 400 hundred years. The greater the difference between the local reservoir age (or 400 years, respectively) and the true reservoir age, the larger the offset between B-P/projection age and ideal/ventilation age will be. This is the reason why the ideal age is close to the projection/B-P age in the north Atlantic where local reservoir age, global mean reservoir age and true reservoir age are similar (Figure 4a). In contrast the ideal age is much smaller in the Pacific (Figure 4b), where the applied reservoir-age correction is smaller than the true one for this source region.

[28] The second factor is that deep water parcels which started to decay at different times in the past and with different initial ^{14}C concentrations are continuously mixed, while ^{14}C decays exponentially during this same time. This nonlinearity makes it impossible to eliminate this mixing source of error completely, but there are attempts to estimate the North Atlantic and Southern Ocean mixing fractions (section 4.2.2). The more mixing between water masses of different ages that occurs, the larger this error will be. Thus, mixing causes little uncertainty close to deepwater formation sites and larger errors further away from them. In reality, we always find a combined effect of reservoir age and mixing errors that are difficult to separate.

[29] The comparison of the ^{14}C age (Figure 1b) with the ideal age (Figure 1a) offers the opportunity to calculate the real offset between these ages. In the deep Atlantic, below 2000 m depth, there is a minimum age offset of around 500 years (Figure 6b). This offset is the result of North Atlantic deepwater formation, where the surface water reservoir age is approximately ~400 years, and entrainment of older local deep waters during sinking [*Adkins and Boyle*, 1999]. With increasing ideal ages and southward movement of the water mass in the Atlantic, the offset reaches up to ~750 years, which represents mixing with Southern Ocean source water. Reservoir ages in the deepwater formation areas of the Weddell Sea and Ross Sea are ~1000 years because of their short surface-residence time [e.g., *Broecker and Peng*, 1982; *Bard*, 1988] that does not allow for a "reset" back to ~400 years such as in the North Atlantic.

[30] In contrast, the offset is nearly equal at 750 years over the whole Pacific below 2000 m depth (Figure 6a). This indicates a well-mixed water mass with roughly equal contributions from the North Atlantic and the Southern Ocean end-members. Thus, the model suggests that ^{14}C ages would be much closer to ventilation ages, if we would correct the deep Pacific $\Delta^{14}C$ for a reservoir age of ~750 years instead of the global mean of 400 years or a local surface ocean age. We will continue to discuss this approach in the context of transient $\Delta^{14}C_{atm}$ variations.

4.2. Transient Atmospheric $\Delta^{14}C$ Variations

[31] The initial projection age increase, when $\Delta^{14}C_{atm}$ starts to decrease (Figure 4), is related to the difference between ideal ages and ^{14}C ages. If the projection to the atmospheric curve is done first and the reservoir age correction afterward, the projection curve intersects with the atmospheric curve too far in the past. For example, if one chooses a location in the deep northern North Pacific with an ideal age of ~1500 years, the ^{14}C age at the same location will be ~2200 years. This way the intersection point would be on the flat part of the atmospheric curve when the deep sea starting point of the projection is already decreasing because the 700 years reservoir age correction is done after the projection.

[32] The opposite happens at the time of the atmospheric pulse: when the deep ocean $\Delta^{14}C$ already starts to increase while the projection curve still intersects with a decreasing part of the atmo-

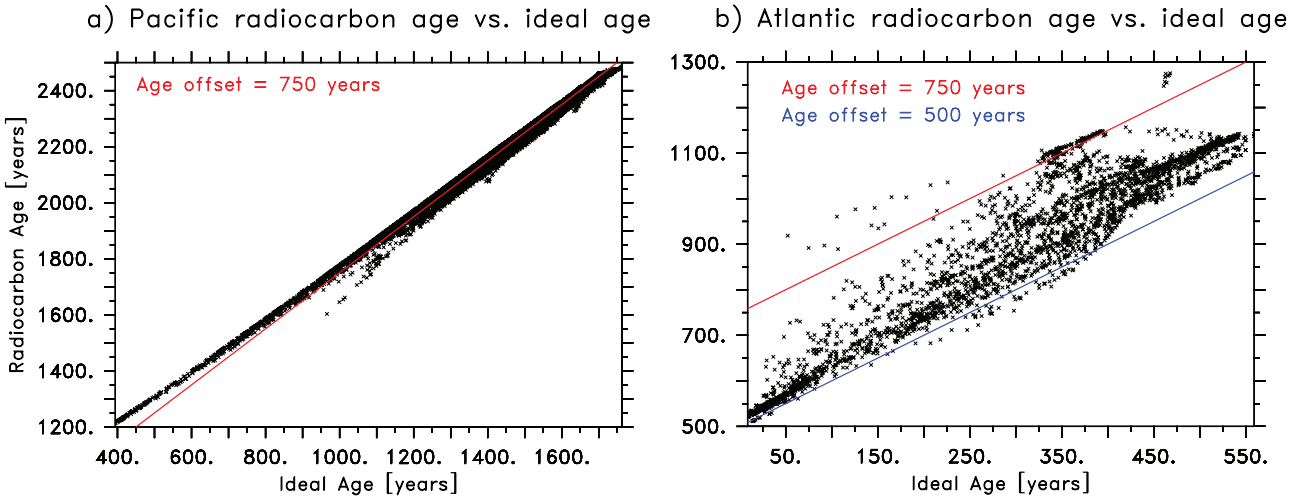

Figure 6. The points mark the offset between ^{14}C age and ideal age in (a) the Pacific and (b) the Atlantic below 2000 m depth. The age offset of around 500 years in Figure 6b especially at low ideal ages is the result of North Atlantic deepwater formation. At higher ideal ages some locations line up at an offset of 750 years, indicating a Southern Ocean source. Most locations, which are not close to the deepwater formation areas, fall in between these two offsets and represent a mixing of the sources. In the whole deep Pacific the offset is nearly the same, about 750 years. The model suggests that ^{14}C ages would be much closer to ventilation ages if we would correct the deep Pacific $\Delta^{14}C$ for Southern Ocean surface water instead of the local one.

spheric curve, the projection ages decrease. The amplitude of the projection age variation is a function of the amplitude of the deep ocean reaction to the pulse. This response is a combination of mixing effects and reservoir age variations. Another difference to *Adkins and Boyle* [1997], which appears to be of minor importance, is that the $\Delta^{14}C$ at this location is not only influenced by advective transport. Due to mixing and diffusion the deep water changes faster than the advection timescale alone would suggest.

[33] The B-P age curve in Figures 4a and 4b shows the same initial drop as the B-P age curve in Figure 1f of *Adkins and Boyle* [1997]. However, in Figure 4b the B-P age in the Pacific curve continues to drop while the Atlantic one in Figure 4a and the curve in Figure 1f of *Adkins and Boyle* [1997] nearly level out after one ventilation age period. *Adkins and Boyle* [1997] assume a closed system in which a deepwater flow is similar to advection in a pipe. Obviously this is nearly valid for the chosen Atlantic location in the UVic ESCM, but it is not the case for the Pacific location, which is far away from a deepwater formation area and cannot react quickly to atmospheric variations due to damping by the large volume of the ocean and mixing processes.

[34] These processes are also influencing the projection ages but to a lesser degree than other uncertainties. Besides the intersection of the curves too far back in time, projection ages are influenced by reservoir-age changes that are not accounted for.

4.2.1. Effect of Reservoir-Age Variations

[35] B-P as well as projection age calculations are affected by temporal and spatial variations in the reservoir age. Reservoir-age variations can be caused by changes in the atmospheric ^{14}C production rate, which result in rapid $\Delta^{14}C_{atm}$ changes [*Laj et al.*, 2002]. Several thousand years of time would be needed to bring the large, slow responding oceanic ^{14}C reservoir to an new equilibrium state. Until a new equilibrium is reached or as long as the ^{14}C-production rate is still changing, reservoir ages will also vary (see Figure 5). Another reason for reservoir-age variations are ocean circulation changes. Both reasons can cause variations of several hundred years, e.g., as reconstructed for the last deglaciation [e.g., *Cao et al.*, 2007; *Sarnthein et al.*, 2007] or modeled for the last 45,000 years [*Franke et al.*, 2008]. Here, we focus on changes in the atmospheric ^{14}C production, because ocean circulation changes are not simulated.

[36] To assess "true" reservoir ages corresponding to a subsurface water parcel, the following information would be required: A surface reservoir-age distribution for the time period of interest and the

source region of the subsurface water parcel. As the knowledge about past surface reservoir ages is very scarce, temporal reservoir-age variations (Figure 5) are not taken into account in the original projection-age method. When using a constant reservoir age, projection ages have an advantage compared to B-P ages in regions where reservoir-age variations are small compared to the ventilation age. Because the planktonic surface ocean ^{14}C value is used in the calculation, B-P ages implicitly consider the local surface-ocean reservoir age. As discussed by *Adkins and Boyle* [1997], the disadvantage of this method is that B-P ages contain a time lag, but they take the reservoir-age variation partly into account. This is an advantage if reservoir ages change over a longer period in the same direction than the ventilation ages. In regions where the time lag is small in relation to the reservoir-age variations (e.g., in the northern North Atlantic), $\Delta^{14}C_{atm}$ variations will influence B-P ages less than projection ages. On the one hand, when atmospheric $\Delta^{14}C$ decreases (or increases) faster than in this simulation, the reservoir-age variations become larger, which would give an advantage to the B-P age method. On the other hand, in this scenario the error introduced by the time lag is also becoming larger, giving the projection-age method an advantage. Due to these opposing effects, both methods become less reliable the faster an atmospheric $\Delta^{14}C$ change occurs.

4.2.2. Effect of Ocean Mixing

[37] Mixing affects both the B-P age and projection age method. It can be divided into two processes in this context. The first is damping of the atmospheric pulse by limited atmosphere-ocean gas exchange and by diffusion in the deep sea; in this sense the ocean operates like a low-pass filter. The second is mixing of water masses with different initial ^{14}C ages. Both processes together (simply called "mixing" in the following) lead to a subsurface ocean $\Delta^{14}C$ time evolution that is a smoothed version of the atmospheric one, e.g., the deep Pacific $\Delta^{14}C$ in Phase 2 is hardly increasing relative to the simulated atmospheric pulse (Figure 3b). If the temporal evolution of the subsurface ocean is not parallel to the surface ocean, both methods are affected by the diverging or converging curves (Figure 3).

[38] An idea to remove the consequences of water mass mixing was proposed by *Adkins and Boyle* [1999]. Measurements of conservative tracers which have different end-member values at the two main deepwater formation sites in the northern North Atlantic and the Weddell/Ross Sea can be used to estimate the fraction that each site contributes at a specific location. For the ^{14}C distribution in the present-day ocean this has been done using phosphate [*Matsumoto*, 2007]. Reconstructions of conservative tracers such as salinity would allow one to do the same for the past if variations of the end-members are also reconstructed.

[39] Following this approach, modeled deep sea ^{14}C of the Atlantic Ocean was plotted against the conservative tracer salinity (Figure 7a). In the North Atlantic with a salinity of 35 psu ^{14}C ages of 500 years were simulated. Moving southward from the northern North Atlantic salinity decreases the more both water masses mix. At the same time ^{14}C decays as long as the water is isolated from the surface. Between a salinity of 35 psu and 34.9 psu there is a steep, nearly linear age increase. This represents the North Atlantic deepwater mass, which fills most of the northern Atlantic. The highest ^{14}C ages are reached in the eastern basin of the southern Atlantic down to Walvis Ridge. In the Atlantic sector of the Southern Ocean with a salinity of around 34.6 psu, the age of the oldest water ranges between 1100 and 1300 years (Figure 7a), although Figure 7b shows that this is freshly-ventilated, "young" water. Most of the ^{14}C signal in the western basin of the Atlantic ocean is due to end-member mixing and not due to water mass aging. The difference between conservative mixing alone and the actual ventilation values are about the same for both the ideal ages and radiocarbon ages (Figure 7). This is a promising result for being able to "unmix" radiocarbon signals from the past ocean and better constrain the "age" of past water masses.

4.3. Assessing Potential Sources of Error

[40] The ocean circulation in our model simulations is time-independent. Possible errors due to variable mixing processes or water mass distribution in the past (e.g., of North Atlantic Deep Water and Antarctic Bottom Water in the North Atlantic [*Skinner and Shackleton*, 2004; *Robinson et al.*, 2005]) are not explored.

[41] As shown for the reservoir age, the results are strongly dependent on the $\Delta^{14}C_{atm}$ variations. If the $\Delta^{14}C_{atm}$ decrease is faster, the subsurface, surface ocean and atmosphere $\Delta^{14}C$ curves converge faster. The system is further away from equilibrium because the decay of ^{14}C is too slow to follow the $\Delta^{14}C$ in the atmosphere. Periods of such fast $\Delta^{14}C_{atm}$ decrease occurred during the last deglaciation. In this case, mixing will become less

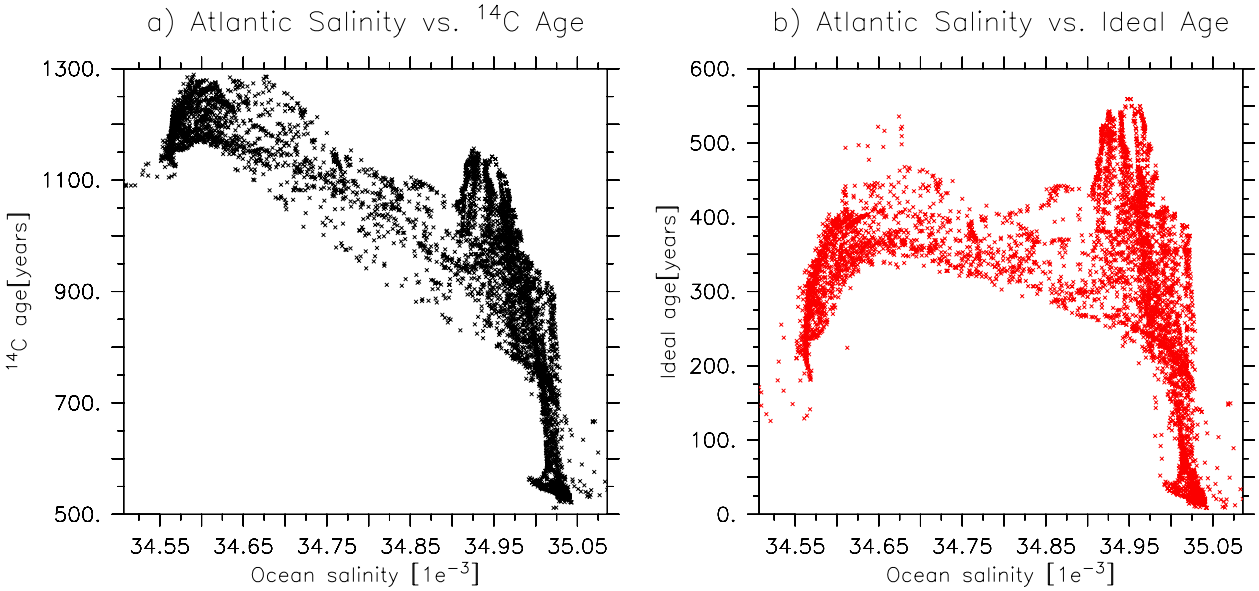

Figure 7. (a) Modeled ^{14}C age versus salinity in the Atlantic Ocean (65W–20E, 65N–80S) between 2000 and 4000 m depth. (b) Modeled ideal age versus salinity for the same region.

important compared to the overall projection-age shift. In contrast, during periods of quite stable $\Delta^{14}C_{atm}$ and surface reservoir ages, mixing will be the important error source in the ventilation age estimation. Thus, it would not make sense to quantify error sources in detail for a particular model simulation, because the relative contributions to the overall error will vary in any single case. Steady-state and transient ^{14}C results are very different from each other and require different approaches when trying to constrain past ventilation rates. Although we are far away from a worst case model scenario and do not involve the complicated natural $\Delta^{14}C_{atm}$ evolution with much more variations, we already see offsets in the projection and B-P ages of up to 400 years in the Pacific compared to the control run.

[42] In the North Atlantic both methods work similarly well, which is in agreement with *Skinner and Shackleton* [2004]. In the model simulation the B-P age method appears to be superior because the time lag between the surface and the deep ocean is small (Figure 3b). Mixing of different water masses is of minor importance at this location as long as the character of the ocean circulation does not change. Thus, taking the reservoir-age variations into account via the planktonic age is an advantage.

[43] In the Pacific both methods have large uncertainties of similar magnitude. The B-P ages are influenced by the time lag between the occurrence of an atmospheric signal in the surface and its arrival in the deep ocean. Reservoir age variations and the projection to an atmospheric $\Delta^{14}C$ too far back in time are the main error sources in the projection-age method.

[44] In our model simulation both methods have small uncertainties close to deepwater formation zones and in time periods and regions of little reservoir-age variations. They have large uncertainties with respect to true ages where deep water has been isolated from the surface for a long time and in time periods of fast $\Delta^{14}C_{atm}$ changes.

4.4. Improved Projection-Age Method

[45] The projection ages constructed from the intersection with the model $\Delta^{14}C$ evolution of the local surface ocean (cyan curve in Figure 3) are at all times and locations less influenced by $\Delta^{14}C_{atm}$ variations than either the original projection ages or the B-P ages, although mixing and taking the "local" instead of the "true" reservoir age into account still causes projection-age variations.

[46] Hence the most important improvement on the original projection-age method is the replacement of the atmospheric $\Delta^{14}C$ curve by a marine $\Delta^{14}C$ reconstruction. This solves the problem of the projection too far into the past as well as an additional error source, which has not been mentioned yet. The atmospheric $\Delta^{14}C$ curve (e.g., INTCAL04 [*Reimer et al.*, 2004]) has many high-frequency variations in the time period where it is

based on tree-ring analysis. These will cause errors in the calculated projection ages because the surface ocean reacts more slowly than the atmosphere to ^{14}C production-rate changes and therefore its $\Delta^{14}C$ evolution is smoother than the atmospheric one.

[47] An alternative way to compute projection ages would therefore be to use reconstructions of the tropical surface ocean $\Delta^{14}C$ as applied by *Skinner and Shackleton* [2004] or the mean ocean surface $\Delta^{14}C$ curve MARINE04 [*Hughen et al.*, 2004] which was chosen by *Cook* [2006]. This fundamental correction can be accomplished with the present state of knowledge but uncertainties concerning the specific reservoir-age variations in the source regions remain.

[48] In order to take them into account, ^{14}C reservoir ages have to be reconstructed at the key locations for deepwater formation in the North Atlantic and the Southern Ocean. A first step would be the focus on the three key circulation states: PD-like, LGM-like and Heinrich-like [*Sarnthein et al.*, 1994; *Alley and Clark*, 1999] before continuous records of submillennial resolution become the objective in the long term. Several approaches offer possibilities to reach this goal: (1) Planktonic foraminifera recorded surface ocean $\Delta^{14}C$ [e.g., *Voelker et al.*, 2000]. (2) Next to deepwater formation sites benthic foraminifera and cold-water corals recorded deep-sea $\Delta^{14}C$ changes that are closely correlated to surface-ocean $\Delta^{14}C$ variations [e.g., *Skinner and Shackleton*, 2004; *Robinson et al.*, 2005]. (3) Spatial and temporal reservoir-age variations have been simulated using an ocean circulation model [*Franke et al.*, 2008]. Additionally the invention of new methods such as ^{14}C-plateau matching [*Sarnthein et al.*, 2007] offers new perspectives to improve the use of already existing data. Nevertheless, the reconstruction of past reservoir-age variations requires further research especially in the Southern Ocean.

[49] In addition to the variability of the reservoir ages at deepwater formations sites, past changes in water mass end-member mixing proportions need to be determined. This requirement can be obtained by conservative tracer reconstructions as suggested by *Adkins and Boyle* [1999] and *Matsumoto* [2007], or by the calculation of trajectories or transit-time distributions [*Peacock and Maltrud*, 2006] using ocean circulation models.

5. Conclusions

[50] Both, the method of B-P ages as well as the projection-age method, have uncertainties that complicate the interpretation of age variations as true ventilation-age changes. It has always to be checked if the atmospheric ^{14}C production rate could be responsible for the $\Delta^{14}C_{atm}$ variation. It should be considered that the Atlantic is less influenced than the Pacific by damping of the atmospheric variations and the difference between "local" reservoir age and the "true" one of the source region. Therefore Pacific age predictions are more sensitive to atmospheric $\Delta^{14}C$ variations, no matter which method is used.

[51] The original projection-age method [*Adkins and Boyle*, 1997] was oversimplified with regard to reservoir ages and ocean mixing. After some improvements, using an ocean surface $\Delta^{14}C$ curve, new reconstructions of the reservoir-age history in deepwater formation areas and estimates of mixing between northern and southern source water in the past, an improved projection-age method has the potential to show circulation changes based on ^{14}C reconstructions, which are only slightly influenced by atmospheric $\Delta^{14}C$ variations.

Acknowledgments

[52] We greatly appreciate the constructive discussions with Mea Cock and the constructive comments of two anonymous reviewers that greatly helped to improve this manuscript. This work was supported by the Deutsche Forschungsgemeinschaft (DFG).

References

Adkins, J. F., and E. A. Boyle (1997), Changing atmospheric $\Delta^{14}C$ and the record of deep water paleoventilation ages, *Paleoceanography*, *12*, 337–344.

Adkins, J. F., and E. A. Boyle (1999), Age screening of deep-sea corals and the record of deep North Atlantic circulation change at 15.4 ka, in *Reconstructing Ocean History: A Window Into the Future*, edited by A. A. Mix, pp. 103–120, Springer, New York.

Adkins, J., H. Cheng, E. A. Boyle, E. R. M. Druffel, and R. L. Edwards (1998), Deep-sea coral evidence for rapid change in ventilation of the deep north Atlantic 15,400 years ago, *Science*, *280*, 725–728.

Ahagon, N., K. Ohkushi, M. Uchida, and T. Mishima (2003), Mid-depth circulation in the northwest Pacific during the last deglaciation: Evidence from foraminiferal radiocarbon ages, *Geophys. Res. Lett.*, *30*(21), 2097, doi:10.1029/2003GL018287.

Alley, R. B., and P. U. Clark (1999), The deglaciation of the Northern Hemisphere: A global perspective, *Annu. Rev. Earth Planet. Sci.*, *27*, 149–182.

Bard, E. (1988), Correction of accelerator mass spectrometry ^{14}C ages measured in planktonic foraminifera: Paleoceanographic implications, *Paleoceanography*, *3*, 635–645.

Berger, W. H. (1977), Carbon dioxide excursions and the deep-sea record, in *The Fate of Fossil-Fuel CO_2 in the Oceans*,

edited by N. R. Andersen and A. Malahoff, pp. 505–542, Plenum, New York.
Bitz, C. M., M. M. Holland, A. J. Weaver, and M. Eby (2001), Simulating the ice-thickness distribution in a coupled climate model, *J. Geophys. Res.*, *106*, 2441–2464.
Bondevik, S., J. Mangerud, H. H. Birks, S. Gulliksen, and P. Reimer (2006), Changes in north Atlanticradiocarbon reservoir ages during the Allerød and Younger Dryas, *Science*, *312*, 1514–1517.
Broecker, W. S., and T.-H. Peng (1982), Tracers in the sea, technical report, Lamont-Doherty Earth Observatory, Palisades, N. Y.
Broecker, W., M. Klas, N. Ragano-Beavan, G. Mathieu, and A. Mix (1988), Accelerator mass spectrometry radiocarbon measurements on marine carbonate samples from deep sea cores and sediment traps, *Radiocarbon*, *30*, 261–295.
Bryan, K., and L. J. Lewis (1979), A water mass model of the world ocean circulation, *J. Geophys. Res.*, *84*, 2503–2517.
Cao, L., R. G. Fairbanks, R. A. Mortlock, and M. J. Risk (2007), Radiocarbon reservoir age of high latitude North Atlantic surface water during the last deglacial, *Quat. Sci. Rev.*, *26*, 732–742.
Cook, M. S. (2006), The paleoceanography of the Bering Sea during the last glacial cycle, Ph.D. thesis, Mass. Inst. of Technol., Cambridge, Mass.
Duplessy, J.-C., M. Arnold, E. Bard, A. Juillet-Leclerc, N. Kallel, and L. Labeyrie (1989), AMS ^{14}C study of transient events and of the ventilation rate of the Pacific intermediate water during the last deglaciation, *Radiocarbon*, *31*, 493–502.
England, M. H. (1995), The age of water and ventilation timescales in a global ocean model, *J. Phys. Oceanogr.*, *25*, 2756–2777.
Fanning, A. F., and A. J. Weaver (1996), An atmospheric energy-moisture balance model: Climatology, interpentadal climate change, and coupling to an ocean general circulation model, *J. Geophys. Res.*, *101*, 15,111–15,128.
Franke, J., A. Paul, and M. Schulz (2008), Modeling variations of marine reservoir ages during the last 45,000 years, *Clim. Past*, *4*, 125–136.
Gent, P. R., and J. C. McWilliams (1990), Isopycnal mixing in ocean circulation models, *J. Phys. Oceanogr.*, *20*, 150–155.
Hughen, K. A., et al. (2004), Marine04 Marine Radiocarbon Age Calibration, 0–26 cal kyr BP, *Radiocarbon*, *46*, 1059–1086.
Hughen, K. A., S. Lehman, J. Southon, J. Overpeck, O. Marchal, C. Herring, and J. Turnbull (2006), Marine-derived ^{14}C calibration and activity record for the past 50,000 years updated from the cariaco basin, *Quat. Sci. Rev.*, *25*, 3216–3227.
Kalnay, E., et al. (1996), The NCEP/NCAR 40-year reanalysis project, *Bull. Am. Meteorol. Soc.*, *77*, 437–471.
Keigwin, L. D., and M. A. Schlegel (2002), Ocean ventilation and sedimentation since the glacial maximum at 3 km in the western North Atlantic, *Geochem. Geophys. Geosyst.*, *3*(6), 1034, doi:10.1029/2001GC000283.
Laj, C., C. Kissel, A. Mazaud, E. Michel, R. Muscheler, and J. Beer (2002), Geomagnetic field intensity, North Atlantic deep water circulation and atmospheric ^{14}C during the last 50 kyr, *Earth Planet. Sci. Lett.*, *200*, 177–190.
Lynch-Stieglitz, J., et al. (2007), Circulation during the last glacial maximum, *Science*, *316*, 66–69.
Matsumoto, K. (2007), Radiocarbon-based circulation age of the world oceans, *J. Geophys. Res.*, *112*, C09004, doi:10.1029/2007JC004095.
McCave, I. N., B. Manighetti, and S. G. Robinson (1995), Sortable silt and find sediment size/composition slicing: Parameters for paleocurrent speed and paleoceanography, *Paleoceanography*, *10*, 593–610.
McManus, J. F., R. Francois, J.-M. Gherardi, L. D. Keigwin, and S. Brown-Leger (2004), Collapse and rapid resumption of Atlantic meridional circulation linked to deglacial climate changes, *Nature*, *428*, 834–837.
Meissner, K. J., A. Schmittner, A. J. Weaver, and J. F. Adkins (2003), Ventilation of the North Atlantic Ocean during the Last Glacial Maximum: A comparison between simulated and observed radiocarbon ages, *Paleoceanography*, *18*(2), 1023, doi:10.1029/2002PA000762.
Orr, J., R. Najjar, C. Sabine, and F. Joos (2000), Abiotic howto, technical report, Lab. des Sci. du Climat et l'Environ., Commiss. à l'Energie At., Saclay, Gif-sur-Yvette, France.
Pacanowski, R. C. (1995), MOM 2 documentation, user's guide and reference manual, technical report, GFDL Ocean Group, Geophys. Fluid Dyn. Lab., Natl. Oceanic and Atmos. Admin., Princeton, N. J.
Peacock, S., and M. Maltrud (2006), Transit-time distributions in a global ocean model, *J. Phys. Oceanogr.*, *36*, 474–495.
Reimer, P. J., et al. (2004), Intcal04 terrestrial radiocarbon age calibration, 0–26 cal kyr BP, *Radiocarbon*, *46*, 1029–1058.
Robinson, L. F., J. F. Adkins, L. D. Keigwin, J. Southon, D. P. Fernandez, and S.-L. Wang (2005), Radiocarbon variability in the western North Atlantic during the last deglaciation, *Science*, *310*, 1469–1473.
Sarnthein, M., K. Winn, S. J. A. Jung, J.-C. Duplessy, L. Labeyrie, H. Erlenkeuser, and G. Ganssen (1994), Changes in east Atlantic deepwater circulation over the last 30000 years: Eight time slice reconstructions, *Paleoceanography*, *9*, 209–267.
Sarnthein, M., P. M. Grootes, J. P. Kennett, and M.-J. Nadeau (2007), ^{14}C reservoir ages show deglacial changes in ocean currents and carbon cycle, in *Ocean Circulation: Mechanisms and Impacts*, *Geophys. Monogr. Ser.*, vol. 173, edited by A. Schmittner, J. Chiang, and S. Hemming, pp. 175–197, AGU, Washington, D. C.
Schimmelmann, A., C. B. Lange, B. Roark, and L. Ingram (2006), Resources for paleoceanographic and paleoclimatic analysis: A 6,700-year stratigraphy and regional radiocarbon reservoir-age (ΔR) record based on varve counting and ^{14}C-AMS dating for the Santa Barbara Basin, offshore Carlifornia, U.S.A., *J. Sediment. Res.*, *76*, 74–80.
Shackleton, N. J., J.-C. Duplessy, M. Arnold, P. Maurice, M. A. Hall, and J. Cartlidge (1988), Radiocarbon age of last glacial Pacific deep water, *Nature*, *335*, 708–711.
Skinner, L. C., and N. J. Shackleton (2004), Rapid transient changes in northeast Atlantic deep water ventilation age across Termination I, *Paleoceanography*, *19*, PA2005, doi:10.1029/2003PA000983.
Stuiver, M., and H. A. Polach (1977), Discussion reporting of ^{14}C data, *Radiocarbon*, *19*, 355–363.
Stuiver, M., G. W. Pearson, and T. Braziunas (1986), Radiocarbon age calibration of marine samples back to 9000 cal yr BP, *Radiocarbon*, *28*, 980–1021.
Thiele, G., and J. L. Sarmiento (1990), Tracer dating and ocean ventilation, *J. Geophys. Res.*, *C95*, 9377–9391.
Voelker, A. H. L., P. M. Grootes, M.-J. Nadeau, and M. Sarnthein (2000), Radiocarbon levels in the Iceland Sea from 25–53 kyr and their link to the Earth magnetic field intensity, *Radiocarbon*, *42*, 437–452.
Weaver, A. J., et al. (2001), The UVic Earth System Climate Model: Model description, climatology, and applications to past, present and future climates, *Atmos. Ocean*, *39*, 361–428.
Williams, R. G., M. A. Spall, and J. C. Marshall (1995), Does Stommel's mixed demon work?, *J. Phys. Oceanogr.*, *25*, 3089–3102.